PNAS
www.pnas.org

Supporting Information for

Identification of a novel micro peptide and multiple secondary cell genes that modulate *Drosophila* male reproductive success

Clément Immarigeon*[1,3], Yohan Frei[1], Sofie Y.N. Delbare[2], Dragan Gligorov[1], Pedro Machado Almeida[4], Jasmine Grey[2], Léa Fabbro[1], Emi Nagoshi[4], Jean-Christophe Billeter[5], Mariana F. Wolfner[2], François Karch[1], Robert K. Maeda*[1]

[1] Department of Genetics and Evolution, Sciences III, University of Geneva, 30 Quai Ernest-Ansermet, 1211 Geneva 4, Switzerland

[2] Department of Molecular Biology and Genetics, Cornell University, Ithaca, New York 14853-2703.

[3] Current affiliation: Molecular, cellular and developmental biology (MCD) Unit, Centre de Biologie Intégrative (CBI), Université de Toulouse, CNRS, Bat 4R4, 118 route de Narbonne, F-31062, Toulouse, France.

[4] Department of Genetics and Evolution, Sciences III, University of Geneva, 30 Quai Ernest-Ansermet, 1211 Geneva 4, Switzerland

[5] Groningen Institute for Evolutionary Life Sciences, University of Groningen, PO Box 11103, Groningen 9700 CC, The Netherlands

* Robert K. Maeda and Clément Immarigeon are corresponding authors.
Email: robert.maeda@unige.ch ; clem.immarigeon@gmail.com;

This file includes:

Figures S1 to S6 and their legends
SI Methods
SI references that do not appear elsewhere in the manuscript

Other supplementary materials (not in this file) for this manuscript include the following:

Datasets S1 to S5

Supplementary Figures

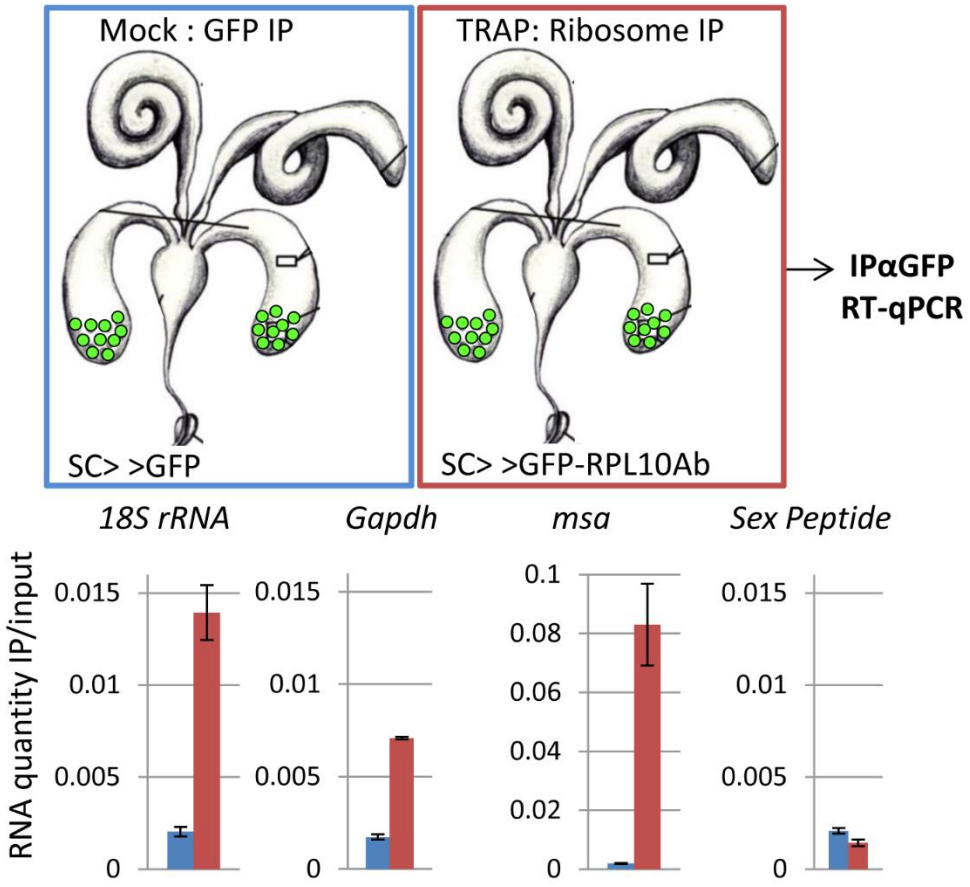

Figure S1: Secondary cell TRAP validation.

A drawing of *Drosophila* male reproductive tracts with GFP-expressing SCs (modified from J. Sitnik (1)). Blue color denotes the control (mock) experiment where only GFP was expressed in the SCs, while red color denotes the TRAP experiment where a GFP-tagged ribosomal protein was expressed in SC (GFP-RPL10Ab (2)). RNA quantifications by real time-qPCR are shown for informative genes, normalized to their respective inputs. *18S rRNA* enrichment shows that ribosomes were successfully enriched, and *Gapdh* enrichment confirms that mRNAs stay bound to ribosomes during the procedure. *msa* strong enrichment shows that *msa* RNA is associated with ribosomes in secondary cells (SCs). *SP* mRNA is not enriched, consistent with its expression only in main cells.

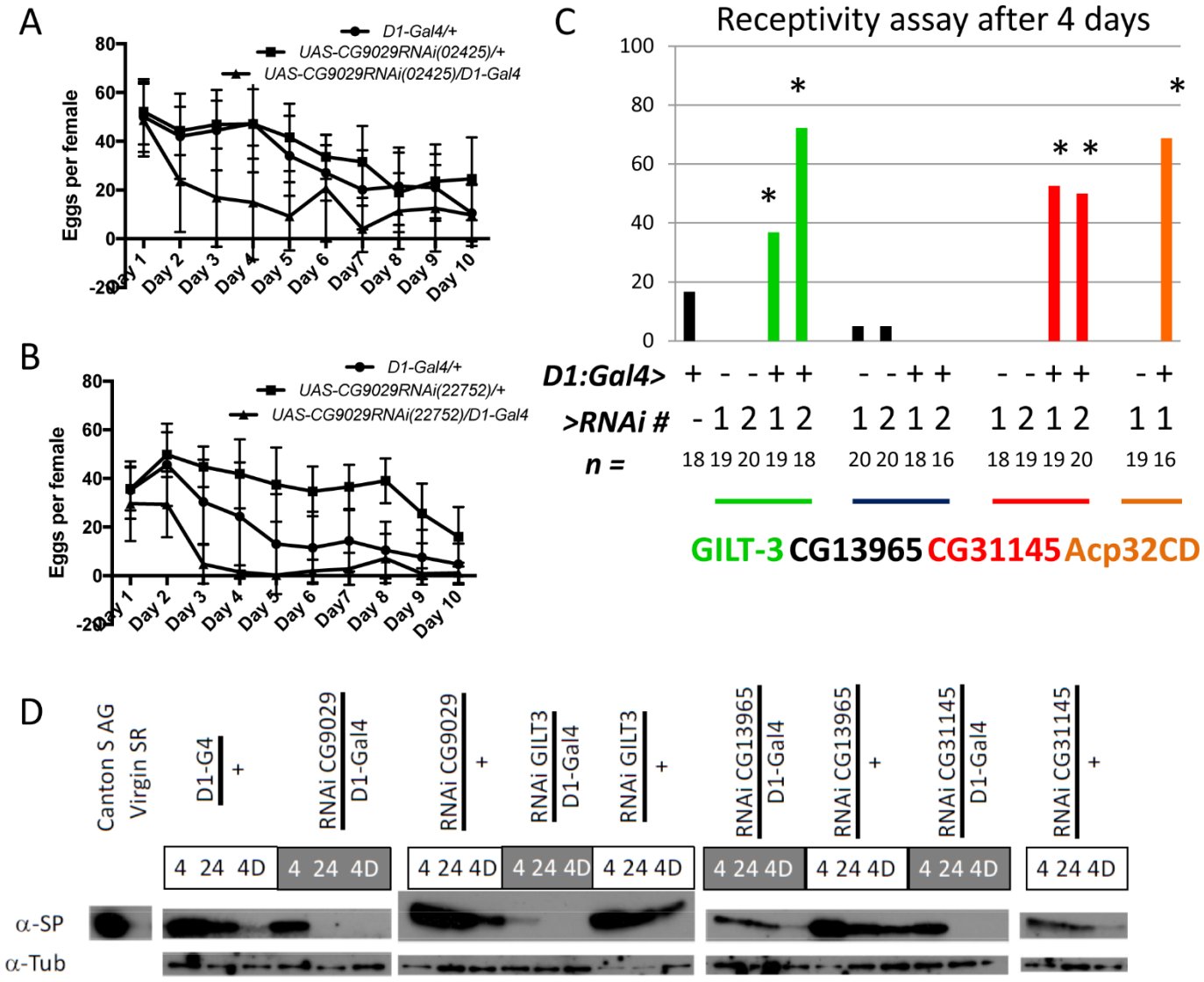

Figure S2: Initial survey of uncharacterized SC signature genes reveals PMR phenotypes.

A. and B. Egg-laying assays using two different RNAi lines targeting CG9029. Approximately 20 males of the genotypes listed were singly mated to individual *Canton S* females. Males were removed after mating and the females transferred every day to a fresh tube over a period of ten days. The eggs laid by each female were counted daily and the average number of eggs per female per day are shown on the graph with standard deviation. The results for the line TRiP HMS02425 are shown in A. and results for the line TRiP HMJ22752 are shown in B. Two-way ANOVA was performed on each pair of curves. For both lines, the RNAi/D1:GAL4 genotype was found to be significantly different from both control (A. $p < .0001$ for both control lines, and for B. $p = 0.0003$ vs D1-G4/+ and $p < 0.0001$ vs RNAi/+). Multiple t-tests were used to determine at which day the lines begin to differ significantly. TRiP HMS02425/D1:GAL4 showed significant differences on days 2-5 and 7 vs D1:GAL4 control ($p = 0.005$ for day 2 and $p < 0.001$ for days 3-5 and 7) and days 2-5, 7 and 10 vs RNAi/+ controls ($p = 0.004$ for day 10 and $p < 0.001$ for the day 2-5 and 7). TRiP HMJ22752/D1:GAL4 showed significant differences on days 2-4 and 7 vs D1:GAL4 control ($p = 0.003$ for day 2 and $p \leq 0.001$ for days 3-4 and 7) and days 2- 10 vs RNAi/+ controls ($p < 0.0001$ for days 2-10).

C. Four-day receptivity assays on *Canton S* females mated individually with male flies of the genotypes listed below the graphs. Remating was scored for 2 hours. Candidate genes were specifically knocked down in SCs using the GAL4-UAS system [84], using 2 different UAS-RNAi lines to avoid false positive results due to potential off target effects. The * highlight the significant differences between the *D1:Gal4/UAS-RNAi* lines and both control lines (*D1:Gal4/+* and *UAS-RNAi/+*) from the same day (see Material and methods). Number of individual mated females is given as n=.
D. Western Blot analysis of Sex Peptide (SP) stored in female seminal receptacles (SR) at different time points after mating with males depleted for the respective genes in the SCs. 4=4 hours post mating, 24=24 hours post mating, 4D=4 days post-mating.

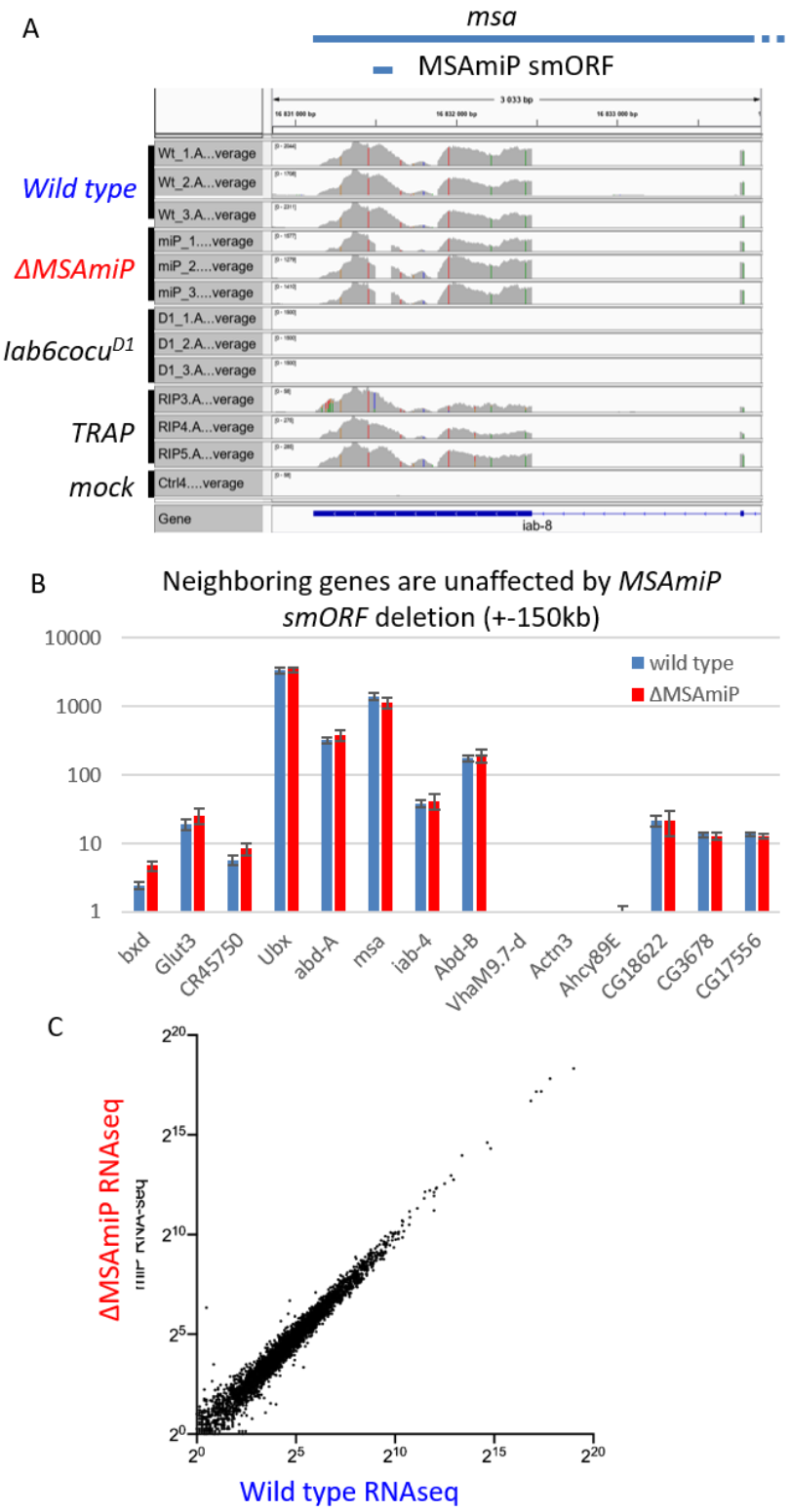

Figure S3: Δ*MSAmiP* secondary cells transcriptome

A. Δ*MSAmiP* is a clean deletion of *MSAmiP smORF* located in the last exon of *msa*. Shown are alignment of RNA reads from multiple datasets to the genomic region containing *MSAmiP smORF.* This deletion has no effect on *msa* expression or stability (nor on neighboring genes expression; see panel B). *lab-6*^{cocuD1} is a null mutant for *msa.*

B. Neighboring genes are unaffected by *MSAmiP smORF* deletion. The genes shown span the whole Bithorax complex genomic locus and beyond, extending >150kb on both sides of the *MSAmiP* deletion. Mean normalized counts are shown on a log10 scale, error bars are standard deviation, for the triplicate replicates.

C. Scatterplot showing gene expression in *wild type* versus Δ*MSAmiP* secondary cells transcriptomes (normalized number of counts per gene, on a log2 scale). Only 6 genes are significantly misexpressed in Δ*MSAmiP* ($p<0.05$), using a General Linear Model, quasi-likelihood F-test with False Discovery Rate (Benjamini & Hochberg) correction to perform statistical analysis of differentially expressed genes. See Dataset S4 for information about these genes.

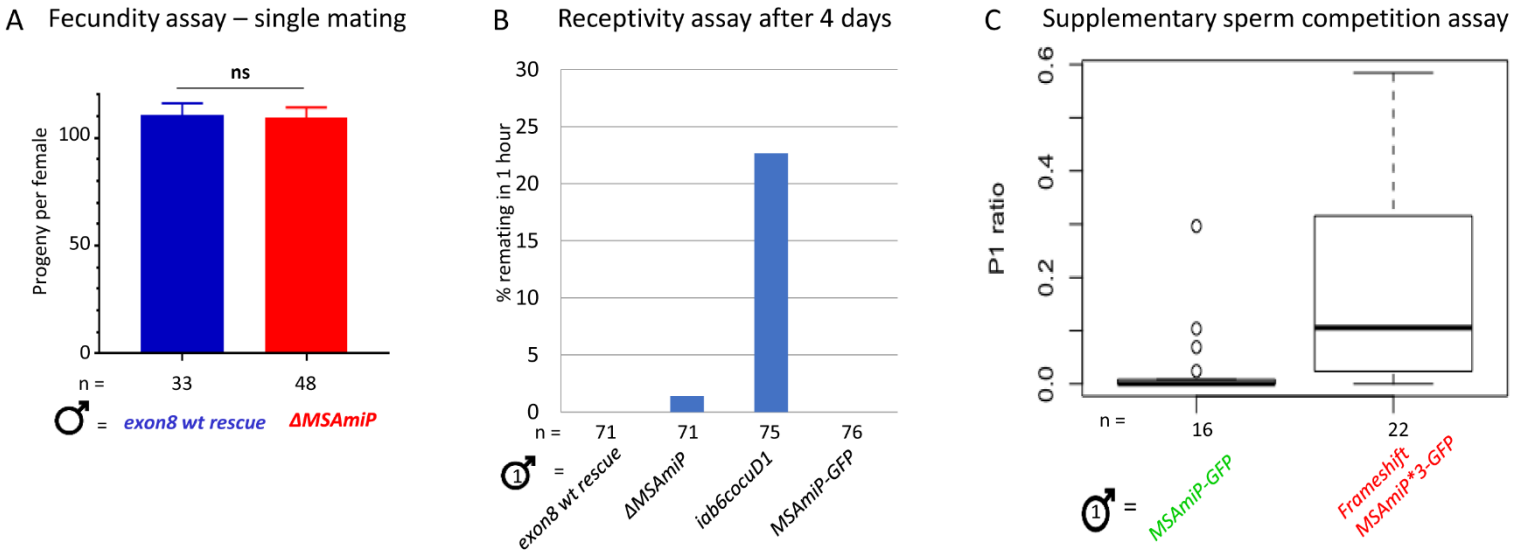

Figure S4: *MSAmiP* mutant males have normal fertility upon single mating and induce proper reduction of female receptivity after mating

A. A fertility assay showing the mean total number of progeny sired by individual *cn bw* females over a 10-day period after a single mating. The genotype of the male is indicated. Statistical tests take replicates into account as random effects and assume a Poisson distribution. The number of offspring is not affected by the genotype of the first male (ns, P=0.9183). The number of individual females observed is shown, as n=, in the figure.
B. A receptivity assay performed on *cn bw* females 4 days after initial mating to males whose genotype is given below the graph. As previously described, *iab6cocuD1* males are unable to decrease female receptivity (1), while neither the *ΔMSAmiP* nor the *MSAmiP-GFP* knock-in significantly differ from the *exon8 wt rescue* control. The number of individual females observed is shown, as n=, in the figure.
C. A sperm competition assay was performed following the setup described in Figure 4A. Results are shown as a bar graph. The black line is the median, the white box shows the range between the first and the third quartile, and the error bars represent 1.5X the difference in the interquartile range (+/-1.5(Q3-Q1)). A statistically significant difference was found between *MSAmiP*3-GFP* and the *MSAmiP-GFP* control (*ANOVA, p= 0.00416*, Wilcoxon Ranked Sum Test, *approximate p<0.0001*). The number of individual females whose progeny were tested is shown, as n=, in the figure.

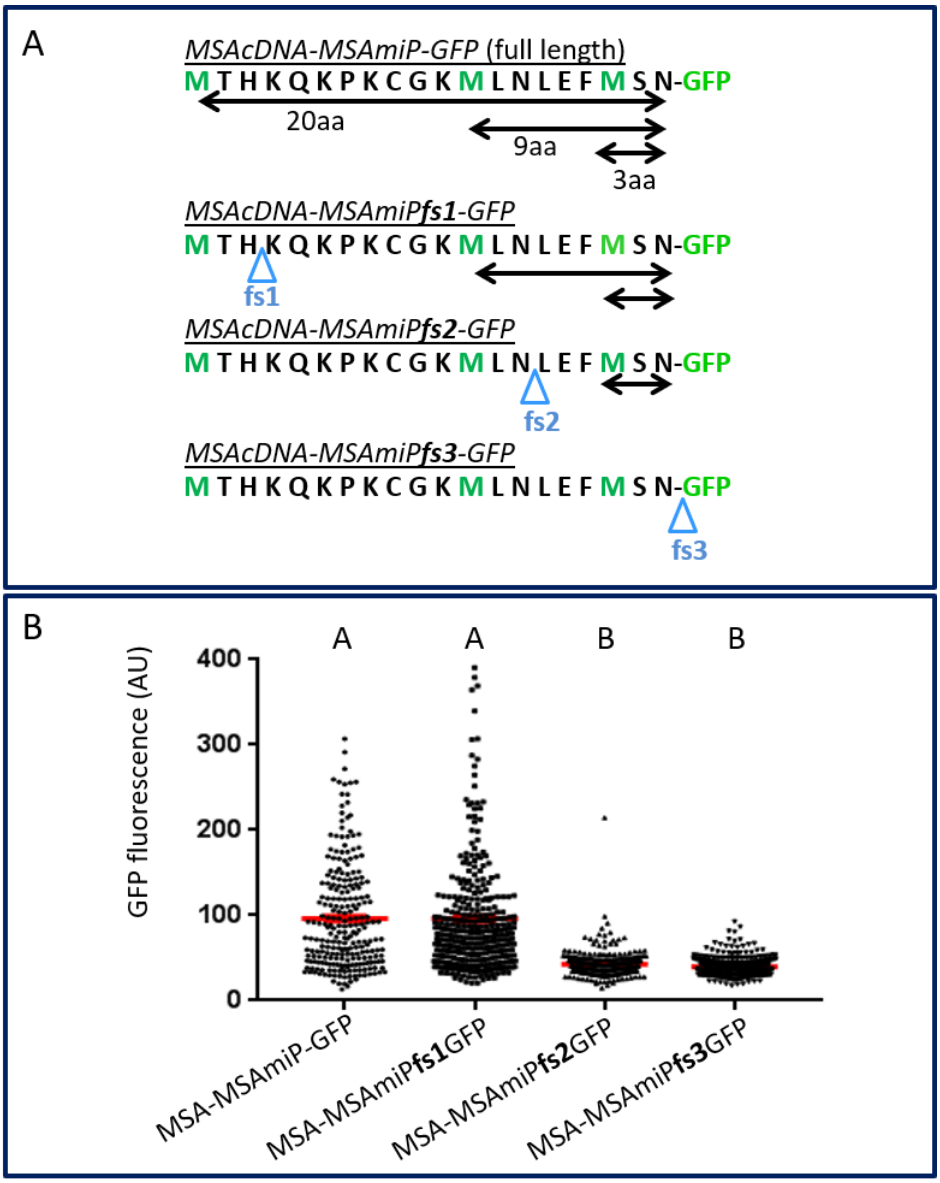

Figure S5: MSAmiP9 is the most abundant peptide encoded by *msa* – a cell-based assay

A. Design of the constructs used to probe for the relative contributions of ATGs in MSAmiP translation initiation. The amino-acid sequence of MSAmiP smORF is shown with methionines highlighted in green (M). Horizontal double arrows represent the different MSAmiP isoforms that might produce a GFP fusion in each construct. Blue triangles labeled fs show the position of the frameshift mutations that we introduced.

B. GFP fluorescence quantified from S2 cells expressing different *MSAcDNA-MSAmiP-GFP* constructs. To quantify GPF fluorescence from a large number of cells, we co-transfected cells with mCherry-alpha-tubulin to identify transfected cells independent of GFP levels. Using Fiji we defined regions of interests (ROI) from confocal z-stacks based on red fluorescence and quantified the green channel from each ROI. Differences between groups were determined by Kruskall-Wallis tests (447.3; $P<0.001$) followed by post-hoc tests comparing all groups. Different letters indicate groups that are significantly different ($P<0.001$) from each other. The number of cells quantified is indicated as n=.

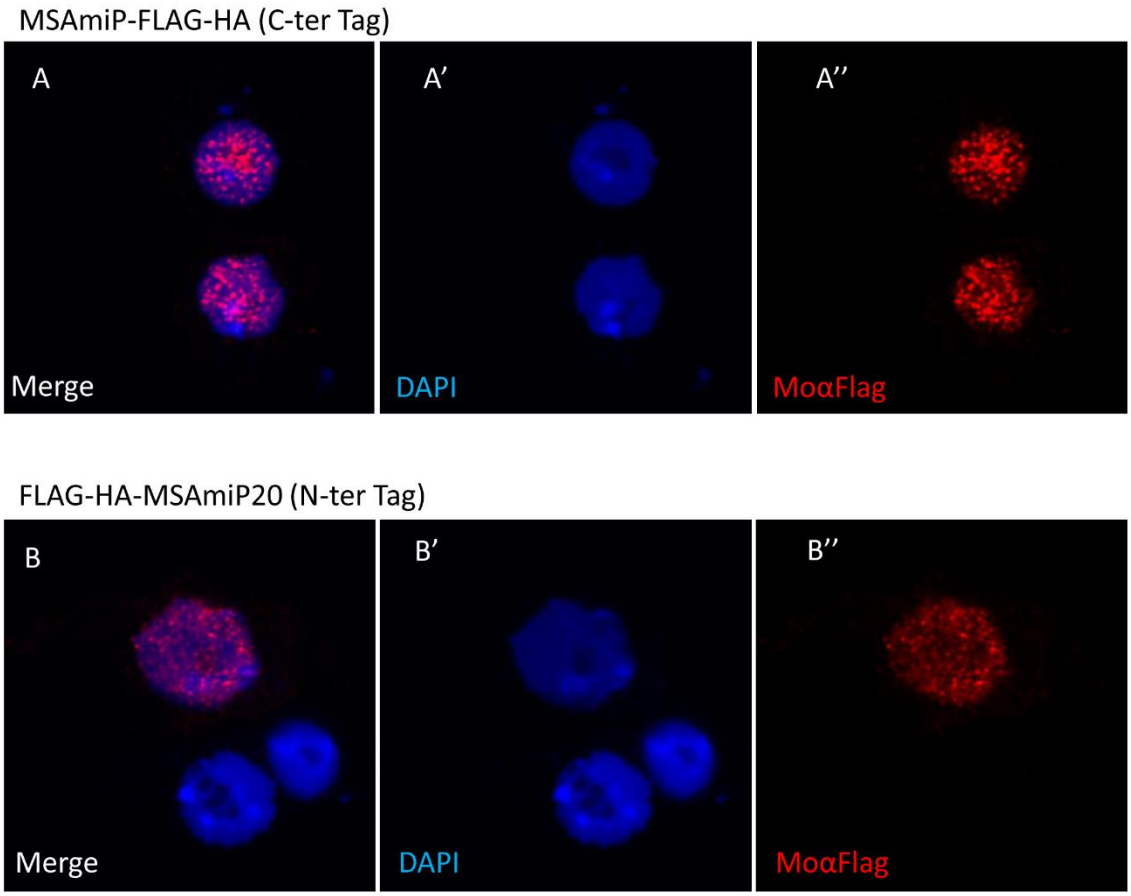

Figure S6: MSAmiP accumulates in cultured S2 cells nuclei

A. and B. Confocal z stack (max projection) of S2 cells transfected with *pActGAL4* + *pUAS-MSAmiP-FLAG-HA* (A) or *pUAS Flag-HA-MSAmiP20* (B) stained with DAPI (blue, nuclei) and anti-Flag antibody (Red).

SI Methods

PCR primers, Gblocks and CRISPR guides
See Dataset S5

Secondary cells sorting and transcriptome
Described in detail in (3).

Translating Ribosomes Affinity purification (TRAP)
We performed TRAP following the protocol from Thomas et al., 2012 (2). The starting biological material was 250 genital tracts (accessory glands + testis + ejaculatory duct) from 5-11 day old virgin males expressing GFP-Rpl10Ab ("TRAP") or GFP ("mock") in SCs. Cell lysis was performed in presence of cycloheximide, which blocks translation elongation – ribosomes are thus stalled on RNAs being translated. Immunoprecipitation was performed overnight at 4°C on a wheel using GFP-Trap agarose beads (Chromotek). Beads were washed three times before proceeding to RNA extraction (MaterPure RNA purification kit, Epicentre). DNase treatment was performed. RNA pellets were resuspended in 10µl TE. 5 µl RNAs were used for Reverse transcription using random hexamers, followed by q-RT PCR (shown for one replicate in Supp Fig 1). Poly-A^+ RNAs from both conditions were sequenced to obtain SC ribosome-associated transcriptome, corrected for background (mock).

NGS, gene counts and data analysis
Each experiment (transcriptome or TRAPseq) was performed in biological triplicates on different days, but libraries and sequencing were all done together. 2ng RNAs from either sorted SCs or TRAP experiments were used to generate cDNAs using polydT primers for reverse transcription and SMARTer technology for amplification (Takara). Libraries for sequencing were prepared using Nextera XT kit (Illumina), and were sequenced using multiplexed, single reads of 100 nucleotides (20-30Million reads per sample). To estimate the artefactual background from TRAP experiment, one mock was also sequenced, using the same volume of starting RNAs as its respective TRAP experiment.
Reads were mapped to the reference *Drosophila* genome (UCSC dm6) using the STAR aligner, and gene count was performed using HTSeq. Genes with fewer than 10 total reads were excluded. The Trimmed Mean of M-values (TMM) method was used to normalize gene counts (4), as it is reported to perform well both with the ability to detect differentially-expressed genes and with controlling false-positives (5, 6). With data having a small number of genes with very high read counts (which is the case of our dataset), TMM performs better than many other normalization methods to control for false positives (7). Differential expression analysis (wild type versus Δ*MSAmiP*) was performed using a General Linear Model, quasi-likelihood F-test with False Discovery Rate (Benjamini & Hochberg) correction.

Plasmid generation:
pUASt mCh alpha tubulin was a gift from C. Seum (8).
pUASt MSAcDNA-MSAmiP-eGFP was constructed by first assembling the exon 8 region with an eGFP marker fused to the 3' end of MSAmiP, still containing the ATG of eGFP. Genomic DNA from a ry^{506} fly was used to PCR amplify the region 5' and 3' of the MSAmiP (with MSAmiP located on the 5' fragment) using the primer pairs ex8_Xho_3900S and miPep_to_Xho_AS for the 5' fragment and miPep_to_Pst_S and ex8_Pst_862_AS for the 3' fragment. Next, eGFP was PCR amplified from the pAc-eGFP plasmid using the pep_eGFP_S and pep_eGFP_AS primers. The three fragments were gel purified and Gibson assembled together with a pGemTeasy vector cut with EcoRI. The eGFP modified exon8 was then PCR amplified using the exon8_fwd and exon8_rev primers. This fragment was then Gibson assembled with a fragment containing MSA exon 1 (amplified from ry^{506} genomic DNA using MSAex1_fwd and MSAex1_rev primers), a fragment containing iab-8 exons 3-7 (also contained in *msa*, amplified from an *iab-8 ncRNA* cDNA clone (from the lab of Welcome Bender, Harvard University, Cambridge, Massachusetts,USA) using the MSA_3-7_fwd and exon3-7_rev primers) and a fragment

containing the pUAST-attB vector cut with EcoRI. The resulting vector was sequenced and integrated into the ZH-68E integration platform (9).
This pUASt-MSAcDNA-MSAmiP-eGFP plasmid was subsequently used to generate derivatives used in Figure S5 probing for the relative contribution of each ATG to translation initiation of MSAmiP. Frameshift point mutations were induced by PCR using degenerate and overlapping primers (see Dataset S5): BamPromF + proper reverse primers was used to generate one fragment, and BampAR + proper forward primer was used to generate the overlapping second fragment. A final PCR was performed using both fragments and the external primers BamPromF + BampAR to generate the mutated full-size fragments that were then digested with BamH1 and ligated into a BamH1-opened pUAStattB plasmid. The ATG of GFP was first mutated and the resulting pUAStattB-MSAcDNA-MSAmiP-GFP was used as template to generate all derivatives with the ATG of GFP mutated, using the same strategy.
PY-endoMSAmiP-GFP plasmid was obtained through NotI + ClaI double digestion of *PY25* (10) removing a fragment of 336 pb containing attP and LoxP. Three DNA fragments were inserted together into the open PY25 vector using Gibson Assembly Cloning kit (NEB): fragment 1 = Gblock1 comprising an attB site and the 3' flanking region to exon 8; fragment "2-GFP" = PCR product 1 obtained using Ex8intraF + Ex8flk3R primers and pUAStMSAcDNA-MSAmiP-GFP as a template; and fragment 3 = PCR product obtained using Flk5LoxPHRF + Ex8IntraR primers on genomic DNA template.
Similarly, *PY25-exon8wt rescue* was obtained by replacing fragment "2-GFP" by fragment "2wt" obtained using Ex8intraF + Ex8flk3R primers on genomic DNA template.
PY25-ΔMSAmiP was obtained by replacing fragment 2 by two fragments "2aΔ" and "2bΔ" obtained by PCR using Ex8intraF + DeltamiPEP-R1 primers and DeltamiPEP-F1 + Ex8flk3R primers, respectively. This results in a 60bp deletion of *MSAmiP* smORF.
PY25-MSAmiP*20-GFP was obtained using Ex8intraF + ATG2+4mutR1 and ATG2+4mutF1 + Ex8flk3R with pUASt MSAcDNA-MSAmiP-GFP as a template.
PY25-MSAmiP*9-GFP was obtained using Ex8intraF + ATG4mutnewR and ATG4mutnewF + Ex8flk3R with pUASt MSAcDNA-MSAmiPfs1-GFP as a template.
PY25-MSAmiP*3-GFP was obtained using Ex8intraF + Ex8flk3R with pUASt MSAcDNA-MSAmiPfs2-GFP as a template.
pUAStattB-*MSAmiP-GFP;* pUAStattB-*MSAmiP-FLAG-HA* and pUAStattB-*FLAG-HA-MSAmiP20* plasmids were obtained inserting the proper fragments A + B (see Dataset S5) into a *pUASt-attB* cut open using EcoR1. They allow expression of tagged version of MSA-miP in transfected S2 cells, and could be readily injected into *PhiC31*-expressing fly embryos for *in vivo* experiments.

Fly stocks:
To sort SCs by FACS, *UAS-GFP* expression was driven in SCs using *AbdB:Gal4* and *D1:GAL4* (1, 11) and the *iab-6*^{cocuD1} mutant (1). For TRAP UAS GFP-RPL10Ab (2) recombined with *D1:GAL4* was used. *UAS-RNAi* lines to test new candidate genes were obtained from the TRiP collection and VDRC collections: *CG9029* RNAi1 = *TRiP HMJ22752* and RNAi2 = *TRiP HMS02425. GILT3* RNAi1 = *102104KK* and RNAi2 = *38069GD*. *CG13965* RNAi1 = *41223GD* and RNAi2 = *106357KK. CG31145* RNAi1 = *108878KK* and RNAi2 = *25036GD. Acp32CD* RNAi1 = *102687KK.*
To generate the ∆*exon8 attP* plateform, CRISPR guides were designed to target regions both upstream (CRISPR3) and downstream of exon 8 (CRISPR6) using the flyCRISPR website (flycrispr.org). These guides were then synthesized on a Gblock (IDT, Coralville, USA) downstream of a U6 promoter as a fusion product with a TRACR/chiRNA fragment. The Gblocks were then cloned into the pGemTeasy vector and co-injected into *y- vasaCas9* embryos together with a PY25-based donor plasmid to delete a 2486 base pair region comprising exon8 as well as flanking sequences on both the 3' and 5' sides. The donor plasmid was obtained by inserting homology regions (HRs) just exterior to the loxP sites flanking the *yellow* marker in a Py25 (10). Each HR corresponds to ~1kb of the sequences flanking exon8 and were obtained by PCR from genomic DNA using the NotI Ex8 320S + Eag ex8 1450ASand MluI Exon8 3970S + AscI ex8 4930AS primers. PCR products were digested with EagI or MluI respectively and cloned into the compatible NotI or AscI unique restriction sites in Py25. The *y*,*vasaPhiC31* chromosome was then introduced into this stock.

After injection, F1 flies with dark yellow^{+} pigmentation appearing from the 2nd abdominal segment (a feature resulting from the insertion of the yellow cassette in the vicinity of *iab-2*). The *yellow* marker was removed using CRE-induced recombination. Subsequent integration of wild type or modified *exon8* regions were obtained by injecting modified PY25 vectors containing an attB site into flies containing this platform and a *vasaPhiC31* transgene. Integrants were selected based on *yellow*$^{+}$ abdomens as before. The *yellow* marker and plasmid backbone was then removed using LoxP sites, leaving only a loxP scar in the genome.
UAS-*MSAmiP-GFP;* UAS-*MSAmiP-FLAG-HA* and UAS-*FLAG-HA-MSAmiP20* lines were obtained through insertion of corresponding pUAStattB plasmids into the *3L 68E attP* plateform (BestGene).
Ex8wt rescue, ΔMSAmiP and *MSAmiP-GFP* stocks were crossed to balancer and isogenic *Cs* lines to put the chromosome III insertions in a similar genetic background before using them in behavior/sperm competition experiments (that is, X, Y and II chromosomes from the isogenic line).

Antibodies:
Antibodies used in the course of this study include: Rabbit anti GFP (Torrey Pines), Mouse anti Flag M2 (Sigma), Rabbit anti HA (Abcam), Rabbit anti-Sex Peptide (12), Goat anti-Rabbit-HRP (Promega, Madison, Wisconsin, USA), Rat anti-Tubulin (ab6160, Abcam, Cambridge, U.K.), Sheep anti-rat-HRP (ab6852, Abcam, Cambridge, U.K.).

Microscopy and GFP fluorescence quantification
Micrographs used in this study were acquired using a Leica SP8 confocal microscope (Figure1, 3, 5 and 6) or a regular fluorescence/phase contrast microscope (Supp. Figure 2E-F). *MSAmiP-GFP* knock-in images are taken from unstained, freshly dissected live glands. Images from Figures 1, 3C and Supp. Figure 6 are maximal projection of multiple confocal z (stack). Images in Figures 3C', C", 5 and 6 are single Z images.

Fluorescence quantification from transfected cells:
We developed an unbiased protocol to quantify GFP fluorescence in a large number of cells that were transfected with different constructs aimed at estimating the relative contribution of each ATG from MSAmiP. S2 cells were co-transfected with a pUAS-*mCherry-α-tubulin* plasmid (8) so we could visualize transfected cells independent of GFP expression (Supp Figure 5). Transfections were performed using Effectene (Qiagen) following manufacturer's recommendation. 1 million S2 cells were transfected with 150ng pAct-GAL4, 150ng pUAS-*mCherry-α-tubulin* and 150ng of one the various versions of pUAS-MSAcDNA-MSAmiP-GFP. Cells were fixed with 4% paraformaldehyde on a coverslip 3 days after transfection. For each condition 3 biological replicates were performed, and quantifications were based on several frames from each replicate. No difference was observed between replicates.
Confocal images of fixed cells were acquired with the same settings, and a Fiji macro was written to automatically define regions of interest: circling red cells (mCherry +) and quantifying green fluorescence in those (GFP). The results are presented in Supp Figure 5 in the form of a scatter plot with mean and SEM (standard error to the mean) so that one can see the variability of GFP intensity for each condition. Despite this variability we could see reproducible trends and statistically significant variations in GFP intensity, thus validating this protocol for relative quantification of GFP fluorescence.

Sperm competition assays:
For the sperm competition assays shown in Fig. S4, we set up single pair matings in vials at room temperature using 3-5 day old virgin *cn bw* females (with white eyes) and 3-5 day old tester males (either MSAmiP-mutant or WT rescue; with red eyes). We observed the matings and removed the male after copulation ended. Females were left in the vial (V1) and, after 3 days, were presented with one 3-5 day old *cn bw* male (white eyes). Females were given a chance to remate over the course of 8 hours, during which time the matings were observed every 15 minutes. If a mating occurred, we waited until copulation ended, then discarded the male and transferred the female to a new vial (V2), in which she could lay eggs for 48h. After 48h, the

female was transferred to V3, and this was repeated up until V5. After spending 48h in V5, females were discarded. Once all progeny had eclosed, we counted the numbers of red eyed offspring (sired by the 1st male to mate) and white eyed offspring (sired by the 2nd male to mate) in V2 to V5. We used these counts to calculate P1, the proportion of offspring sired by the first male to mate (either *ΔMSAmiP* mutant, *exon8wt rescue*, or *MSAmiP-GFP* knock in).
We excluded females from the analysis if they did not produce any offspring during the experiment (5 females from replicate 1 and 3 females from replicate 2). In addition, if a female had a P1 equal to 1 or 0, we verified her P1 value in V1. If P1 in V1 was also equal to 1 or 0, this indicates that 100% of a female's offspring was sired by only the first or only the second male, suggesting that she had mated with only the first or the second male. We excluded these females from the experiment as well. (Even though we observed matings, we did not time them. Thus, it is possible that we observed a male's attempt to mate with a female, but that a mating did not really occur. We did not observe any bias in P1=1 or P1=0 between MSAmiP-mutant or WT rescue.)
The experiment presented in Figure S4C comparing the *MSAmiP*3-GFP* point mutant (n=22) to *MSAmiP-GFP* (n=16) was performed following the procedures described in the Methods section. The females used were from the same *cn bw* line and the food recipe was the same, but the experiments shown in Figure 4B and Figure S4C were carried out two years apart in different institutions, which might explain the observed difference in absolute P1 value obtained for *MSAmiP-GFP* line.

Receptivity Assays:
We set up single pair matings in vials at room temperature using 5 days old virgin *Canton S* females and 5 days old tester males (either from the SC RNAi series shown in Figure 2B / Supp. Figure 2C, and the MSAmiP series shown in Supp. Figure 4B*).* We observed the matings and removed the male after copulation ended. Females were left in the vial and after 4 days, were presented with one 5 days old *Canton S* male. Matings were observed and scored for one hour (Figure 2B) or two hours (Supp. Figure 2C and Sup Figure 4B).
To test the statistical significance of our results shown in Figure 2B, Sup Figure 2C and Sup Figure 4B, we would perform Fisher's exact test for each D1:Gal4/UAS-RNAi line versus both control lines (D1:GAL4/+ and UAS-RNAi/+) from the same day. For CG9029, P-value is ≤ 0.0001 for both RNAi lines versus all controls.
GILT3 RNAi1/D1:GAL4: P= 0.038 vs D1:GAL4/+ and P=0.0004 vs RNAi1/+. GILT3 RNAi2: P-value is ≤ 0.0001 versus both controls. Acp32CD RNAi1/D1:GAL4: P=0.0014 vs D1:GAL4/+ and P<0.0001 vs RNAi/+. CG31145 RNAi1/D1:GAL4: P=0.0025 vs D1:GAL4/+ and p < 0.0001 vs RNAi1/+. CG31145 RNAi2/D1:GAL4: p=0.0089 vs D1:GAL4/+ and p<0.0001 vs RNAi2/+.

Sample preparation for Western blots
For Figure 2C and Supp. Figure 2D: Single pair matings were performed at RT using 5 day old virgin, Canton S females and 3-7 day old males of the following genotypes: D1-G4/+, *HMJ22752 (RNAi CG9029)/D1-G4, HMJ22752(RNAi CG9029)/+,* VDRC *102104KK (RNAi Gilt-3)/D1-G4,* VDRC *102104KK (RNAi Gilt-3)/+,* VDRC *106357KK (RNAi CG13965)/D1-G4,* VDRC *106357KK (RNAi CG13965)/+,* VDRC *108878KK (RNAi CG31145)/D1-G4,* VDRC *108878KK (RNAi CG31145)/+,* VDRC *102687KK (RNAi Acp32CD)/D1-G4,* and VDRC *102687KK (RNAi Acp32CD)/+.* For each male genotype ~60 crosses were set up. The matings were monitored and the times of matings were noted. Mated females were isolated from their mates and snap frozen in liquid nitrogen after 2-4 hours, 24 hours or 4 days after mating. For each timepoint at least 5 females were collected. For each genotype/timepoint, females were dissected and seminal receptacles were isolated and boiled in SDS sample buffer. The equivalent of ~5 female seminal receptacles were run per well of a 16% Tris-Glycine gel (purchased from Thermo Fisher Scientific (Waltham, USA)). Gels were then transferred onto PVDF membranes and probed with anti-Sex Peptide antibodies (1:2000 dilution) and revealed using the Supersignal West Pico chemiluminescence reagents (Thermo Fisher Scientific (Waltham, USA)) after incubation with a goat anti-rabbit-HRP conjugated secondary antibody (Promega, Madison, USA at a 1:5000 dilution). Blots were then stripped using mild stripping buffer following the protocol and recipes from Abcam (abcam.com). The stripped blots were then probed with a rat anti-tubulin antibody (ab6160, Abcam, Cambridge, U.K., at a 1:5000 dilution) and revealed with a sheep anti-rat-HRP

antibody (ab6852, Abcam, Cambridge, U.K. at a 1:5000 dilution) and the Supersignal West Pico kit (Thermo Fisher Scientific (Waltham, USA)).

For Figure 5C: 5 pairs of accessory glands from 1 day old males are loaded for each knock in and wild type lane, 1 pair of glands is loaded for the *da>>MSAmiP-GFP* positive control (*daughterless:GAL4>UAS:MSAmiP-GFP*).

SI References

1. D. Gligorov, J. L. Sitnik, R. K. Maeda, M. F. Wolfner, F. Karch, A novel function for the Hox gene Abd-B in the male accessory gland regulates the long-term female post-mating response in Drosophila. *PLoS Genet* **9**, e1003395 (2013).
2. A. Thomas, *et al.*, A versatile method for cell-specific profiling of translated mRNAs in Drosophila. *PLoS One* **7**, e40276 (2012).
3. C. Immarigeon, F. Karch, R. K. Maeda, A FACS-based Protocol to Isolate RNA from the Secondary Cells of Drosophila Male Accessory Glands. *J Vis Exp* (2019) https:/doi.org/10.3791/60218.
4. D. Bates, M. Mächler, B. Bolker, S. Walker, Fitting Linear Mixed-Effects Models Using lme4. *2015* **67**, 48 (2015).
5. , R : A language and environment for statistical computing. . *R Found. Stat. Comput. Vienna, Austria.* (2018).
6. R. Length, Emmeans: Estimated Marginal Means, aka Least-Squares Means. R package version 1.4.1. (2019).
7. Y. Lin, *et al.*, Comparison of normalization and differential expression analyses using RNA-Seq data from 726 individual Drosophila melanogaster. *BMC Genomics* **17** (2016).
8. C. Montagne, M. Gonzalez-Gaitan, Sara endosomes and the asymmetric division of intestinal stem cells. *Development* **141**, 2014–2023 (2014).
9. J. Bischof, R. K. Maeda, M. Hediger, F. Karch, K. Basler, An optimized transgenesis system for Drosophila using germ-line-specific phiC31 integrases. *Proc Natl Acad Sci U S A* **104**, 3312–3317 (2007).
10. C. Iampietro, M. Gummalla, A. Mutero, F. Karch, R. K. Maeda, Initiator elements function to determine the activity state of BX-C enhancers. *PLoS Genet* **6**, e1001260 (2010).
11. R. K. Maeda, *et al.*, The lncRNA male-specific abdominal plays a critical role in Drosophila accessory gland development and male fertility. *PLoS Genet* **14**, e1007519 (2018).
12. H. Liu, E. Kubli, Sex-peptide is the molecular basis of the sperm effect in Drosophila melanogaster. *Proc Natl Acad Sci U S A* **100**, 9929–9933 (2003).